MODELISATION AND PERFORMANCE EVALUATION OF 5G VEHICULAR NETWORK USING A 3D-MASSIVE MIMO ANTENNA SYSTEM

Randriamiadana Zakasoa Arilova[1], Randriamitantsoa Paul Auguste[2], Randriamitantsoa Andry Auguste[3]

[1] *PhD student, TASI, ED-STII, Antananarivo, Madagascar*
[2] *Thesis Director, TASI, ED-STII, Antananarivo, Madagascar*
[3] *Professor, TASI, ED-STII, Antananarivo, Madagascar*

ABSTRACT

Internet of Things (IoT) is smartly changing various existing research areas into new themes including smart-home, smart-campus, smart-health, smart-industry and smart-transport. Relying on the basis of 'Smart-Transport', Internet of Vehicles (IoV) is evolving as a new theme of research and development. The IoV includes five types of vehicular communications; namely, Vehicle-to-Vehicle, Vehicle-to-Roadside, Vehicle-to-Infrastructure of cellular networks, Vehicle-to-Personal devices and Vehicle-to-Sensors. In addition to that, traditional Massive Multiple-input-multiple-output (Massive MIMO) systems of current telecommunication network are capable of adaptation in the azimuth only. Recently, the trend is to enhance system performance by exploiting the channel's degrees of freedom in the elevation, which necessitates the characterization of 3D channels by the use of 3D-Massive MIMO antenna system. For that, a mathematical model and a performance evaluation of 5G vehicular network using a 3D-Massive MIMO system is presented in this article.

Keyword: *5G, IoT, IoV, 3D-Massive MIMO*

1. OVERALL ARCHITECTURE OF 5G NETWORK

The general architecture of 5G network is composed with a Next Generation RAN(NG-RAN) and a 5G Core(5GC). The Figure 01 illustrate the general architecture of 5G network and the Figure 02 represent the reference point of the system architecture.

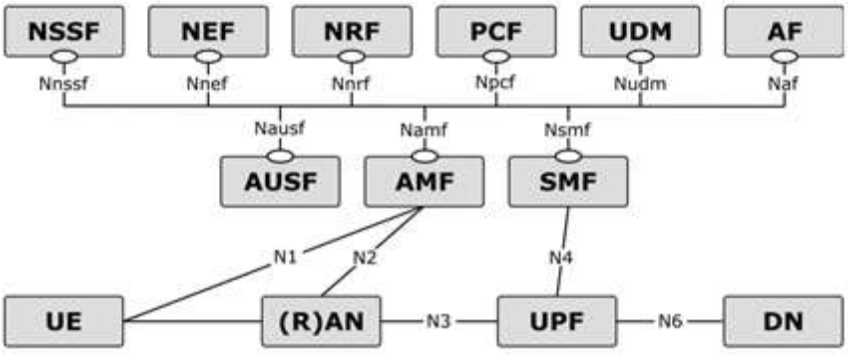

Figure 01: General architecture of 5G network

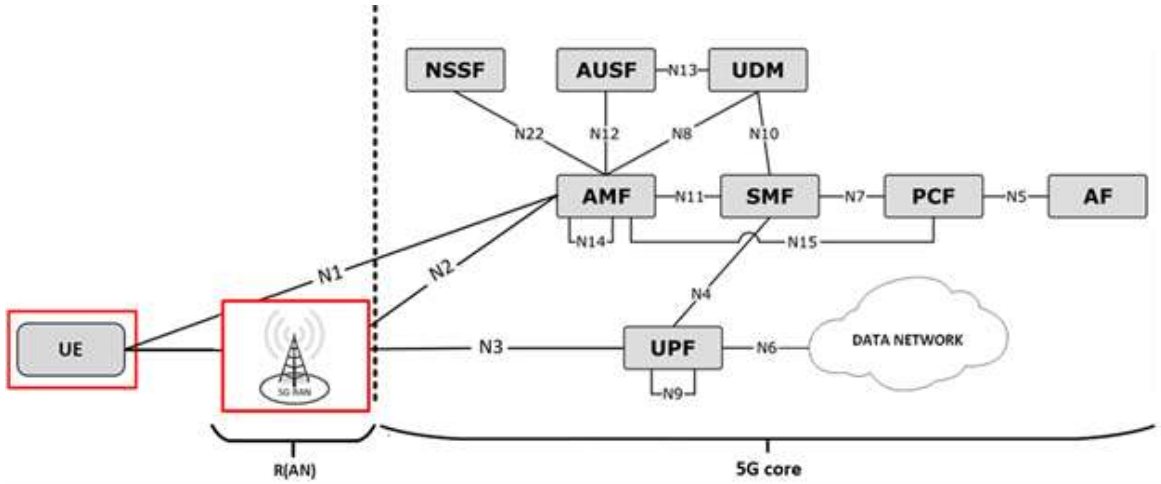

Figure 02: 5G architecture and interface entities

AF: Application Function
AMF: Access and Mobility Management Function (MME)
AUSF: Authentication Server Function
NEF: Network Exposure Function
NEF: Network Exposure Function
NSSF: Network Slice Selection Function
PCF: Policy Control Function
SMF: Session Management Function
UDM: Unified Data Management
DN: Data Network
UPF: User Plane Function (S/PGW)
RAN: Radio Access Network
UE: User Equipment

Our work will focus on the red bloc represented by the Figure 02 and the principles application is the Internet of Vehicle (IoT).

2. OVERALL ARCHITECTURE OF 5G VEHICULAR NETWORK

The Figure 03 bellow show the general architecture of 5G vehicular network.

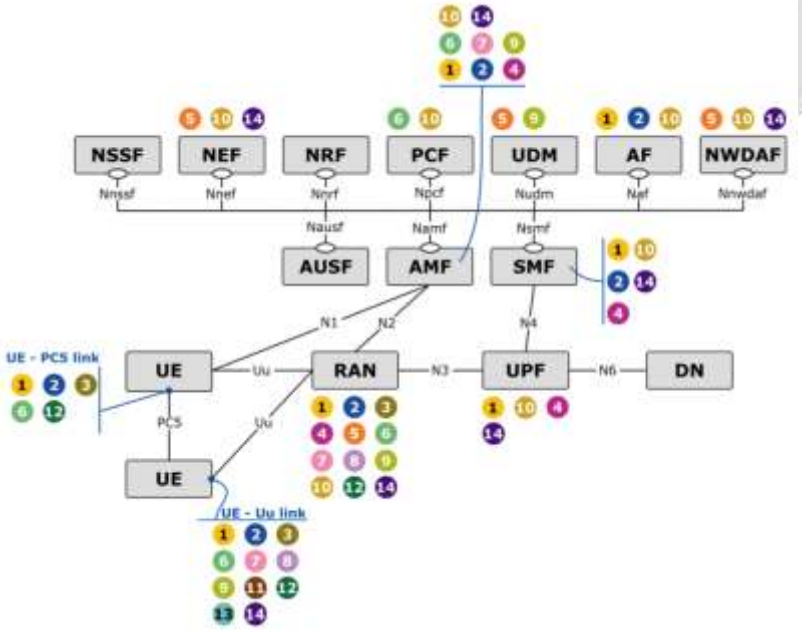

Figure 03: Overall architecture of 5G vehicular network

The complete list of the technical components IoV network architecture represented by the Figure 03 is listed in the Table 01 [2].

Table 01: Architectural technical components of IoV

	Technical components (CT)	Application
1	RSU for Smart Zone (SM-Zone)	Network procedures
2	Fast application-aware setup of unicast SL	Network procedures
3	Multi-connectivité SL and Uu	Multi-connectivity cooperation
4	Location awase scheduling	Network procedures
5	Infrastructure as a Service (IaaS) for vehicular domain	Orchestration and management
6	Redundant mode PC5 and Uu	Multi-connectivity procedure
7	Evolution of infrastructure-based communication for localized V2X traffic	Network procedures
8	Use case-aware multi-RAT, multi-link connectivity	Multi-connectivity procedure
9	Multi operator solutions for V2X communications	Network procedures
10	V2X service negotiation	Network procedures
11	Edge computing in millimeter Wave Cellular V2X networks	Edge-Computing
12	Dynamic selection of PC5 and Uu communication modes	Multi-connectivity cooperation
13	Security and privacy enablers	Point to point security
14	5G core network evolution for edge computing-based mobility	Edge-Computing

3. 5G Vehicular system communication model

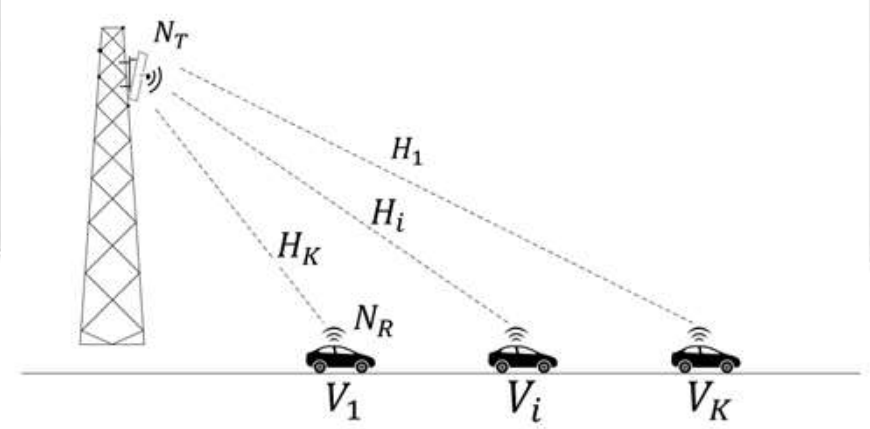

Figure 04: Communication system model for Internet of vehicle

To analyze the performance of 3D-Massive MIMO systems, it is necessary to adopt a frequency nonselective directional Rayleigh fading channel model [1]. The channel impulse response is related to both the complex amplitude and the steering vector components of the antenna arrays. Therefore, the channel impulse response of the 3D vehicular Massive MIMO antenna array model can be expressed as:

$$h(t) = \sum_{j=1}^{N} a_j(t) \cdot v(\beta_A, \beta_E) \quad (1)$$

Where $a_j(t)$ denotes the complex amplitude

$v(\beta_A, \beta_E)$ is the steering vector of the compact antenna array

N is the total number of large-scale antennas

β_A denotes the azimuth angle

β_E denotes the elevation angles

Therefore, the steering vector can be expressed as

$$v(\beta_A, \beta_E) = \left(\begin{bmatrix} 1 \\ e^{jm} \\ e^{j2m} \\ \cdots \\ e^{j(W-1)m} \end{bmatrix} \left[1, e^{jp}, \ldots, e^{j(L-1)p}\right] \right) \quad (2)$$

Where $m = k_w d_x \cos\beta_A \cos\beta_E$

$p = k_w d_y \cos\beta_A \cos\beta_E$

$k_w = 2\pi/\lambda$

λ denotes the wavelength

d_x and d_y denote the respective spacing between the array elements parallel to the x- and y-axes

For the IoV mobile radio environments, we first introduce the proposed 3D vehicle massive MIMO antenna array model, including the spherical wavefront assumption and geometric properties. Here, large-scale omnidirectional antennas are employed at the rooftop of the vehicle. The bottom side of the vehicle is close to the ground. For that, the signals cannot be effectively transmitted by multipath links. We therefore present an approach for vehicles to form a virtual 3D ULA in the shape of a box, wherein large-scale virtual antennas are equally situated on the surfaces of ABCD, EFCD, HGBA, HADE, FGBC, as illustrated in Figure 05.

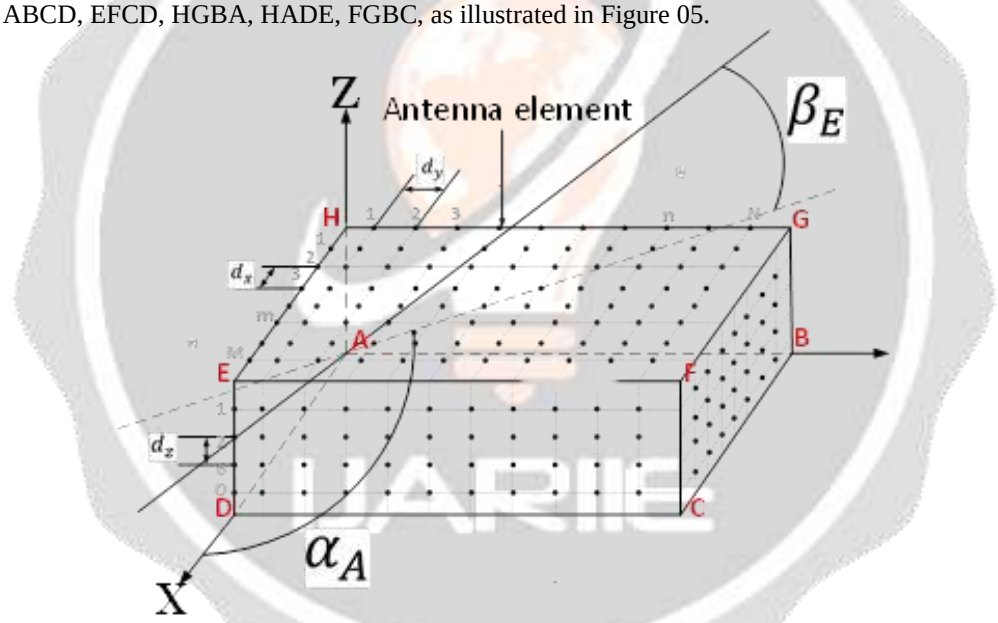

Figure 05: Proposed 3D vehicle massive MIMO virtual antenna array model

From the Figure 05, the steering vector for the proposed model can be expressed as:

$$v(\beta_A, \beta_E) = [v_1(\beta_A, \beta_E), v_2(\beta_A, \beta_E), \ldots, v_{mno}(\beta_A, \beta_E), v_N(\beta_A, \beta_E)]^T \quad (3)$$

Where $v_{mno}(\beta_A, \beta_E)$ denotes the phase steering of the $mno-th$ element for the proposed 3D virtual array model which can be defined as the $m-$, $n-$ and $o-$ th element along with the positive $x-$, $y-$ and $z-$axes, i.e, $m = 1,2,\ldots,$ M, $n = 1,2,\ldots,N$ and $o = 1,2,\ldots O$, as shown in the Figure 05.

4. IoV environments and link types

Radio propagation is influenced by different types of objects found in the environment where the communication occurs. In case of IoV, the most important objects that influence the propagation are buildings, vehicles and different types of vegetation. Different scenarios for IoV channel modelling, link types, vehicle types and main propagation states are described in Figure 06 [2].

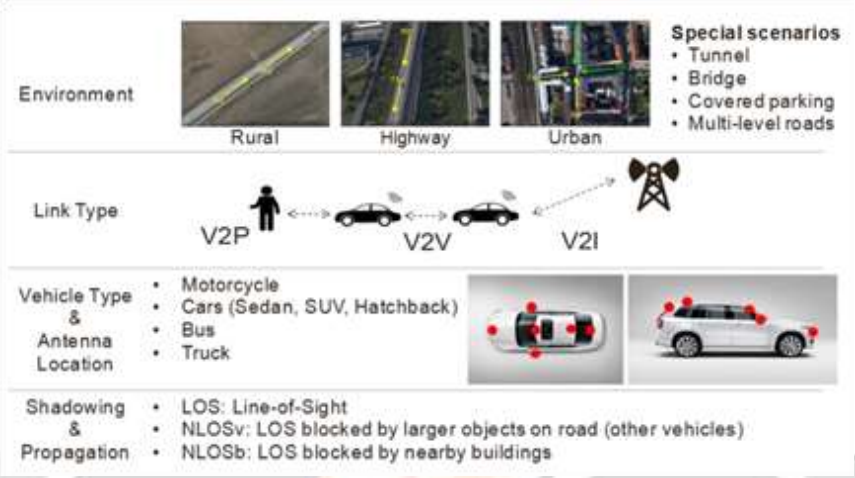

Figure 06: Environments, link types, and specific considerations for IoV channel modelling

5. Channel model for IoV communication

Figure 07 represent the 3D-Massive MIMO antenna element disposition in a vehicle. Here, we proposed that the 3D-Massive MIMO antenna element, which form a 3D-beam, are installed on the rooftop of a vehicle.

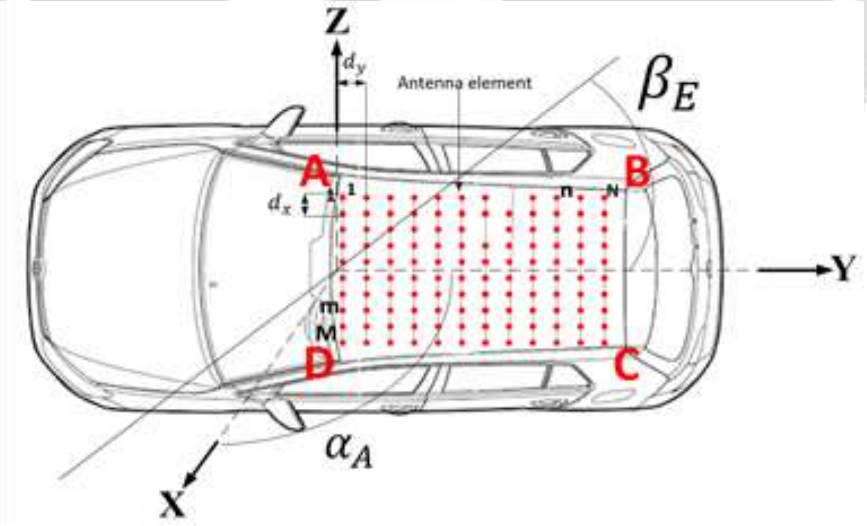

Figure 07: 3D-Massive MIMO antenna element installed in a vehicle

And the Figure 08 represent the reference of the azimuth and elevation angle depending the orientation of the vehicle.

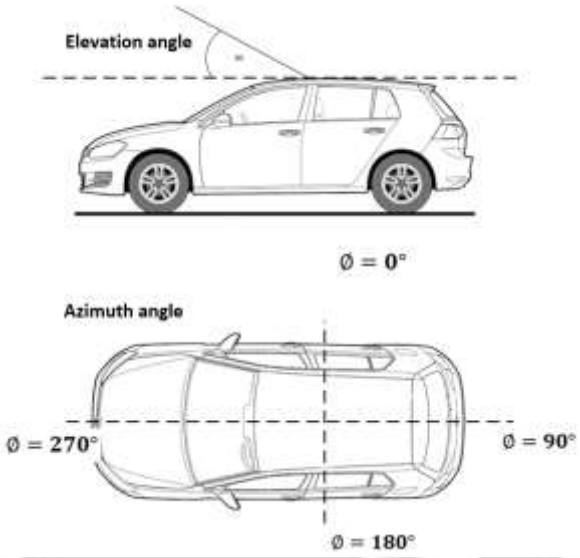

Figure 08: Azimuth and angular representation of 3D-Massive MIMO vehicular system

From the representation of antenna element and the channel transmission, in Figure 04, the matrix channel H(t) with dimension M x N is given by [3]:

$$\mathrm{H(t)} = [h_{N_T N_R}(t,\tau)]_{M\times N} \tag{4}$$

Where $N_T = 1, \dots, M$ is the number of transmitter antenna

$N_R = 1, \dots, N$ is the number of receiver antenna

In the case of a LOS trajectory, the distance between the transmitter and the receiver is given by:

$$d^{LOS}_{n_t,m'n'o'}(t) = \sqrt{(m'd_{x'} - md_x + v_R t\sin\emptyset_v)^2 + \left(o'd_{y'} - od_y + v_R t\cos\emptyset_v\right)^2} \tag{5}$$

And for the case of NLOS trajectory, the distance between the mno^{th} antenna transmitter and the $m'n'o'^{th}$ antenna receiver, for a given time t is given by:

$$d^{T}_{mno}(t) = \frac{1}{2k_1}\times\left(-k_2 + \sqrt{k_2^2 - 4k_1k_3}\right) \tag{6}$$

Where

$$k_1 = b^2c^2cos^2\beta_T cos^2\alpha_T + a^2c^2cos^2\beta_T sin^2\alpha_T + a^2b^2sin^2\beta_T$$

$$k_2 = 2b^2c^2pd_y\cos\beta_T\cos\alpha_T - db^2c^2\cos\beta_T\cos\alpha_T + 2a^2c^2md_x\cos\beta_T\sin\alpha_T$$

And

$$k_3 = \left(\frac{D}{2} - pd_y\right)^2 b^2c^2 + a^2c^2(md_x)^2 + a^2b^2c^2$$

The distance of the $m'n'o'^{th}$ antenna from the scatterer to the mobile terminal can be expressed in terms of the arrival angle. In this case, the expression of the arrival angle α_R and α_R, at the receiver can be replaced by the departure angle α_E and α_E.

Thus, the distance between the $m'n'o'^{th}$ antenna and the mobile terminal is given by:

$$d^T_{m'n'o'}(t) = \sqrt{\left(d^T_{mno}(t)\right)^2 + d^2_{mno,m'n'o'}(t) - 2d^T_{mno}(t)d_{mno,m'n'o'}(t)\cos\beta_T \cos(\alpha_T - \alpha_0)} \quad (7)$$

The impulse response of the IoV channel model, that we can use to characterize the physical properties of the wired environment is a superposition of the multi-path component with different amplitude $a_{l,n_t n_r,n}(t)$, phases $\psi_{l,n_t n_r,n}$ and doppler frequency $f_{d,1,n_t n_r,n}(t)$, EAAD $\alpha_{T_{n_t},l,n}(t)$, EAED $\beta_{T_{n_t},l,n}(t)$, EAAA $\alpha_{R_{n_r},l,n}(t)$ and EAEA $\beta_{R_{n_r},l,n}(t)$.

Related to the base station, the angular position of the user k corresponding to the antenna is represented in form of a vector with a size M x N.
The total number of 3D-Massive MIMO antenna element is given by:

$$N_T = MN + 2NO + 2MO \quad (8)$$

$$a(\alpha_A, \beta_E) = vec\left(\begin{bmatrix} 1 \\ e^{j} \\ e^{j2m} \\ \dots \\ e^{j(W-1)m} \end{bmatrix}\begin{bmatrix} 1, e^{j n_t}, \dots, \\ e^{j(L-1)n_t} \end{bmatrix}\right) \quad (9)$$

Where $m = k_w d_x \cos\alpha_A \cos\beta_E$

$n_t = k_w d_y \cos\alpha_A \cos\beta_E$

$k_w = \frac{2\pi}{\lambda}$

λ represent the wavelength

d_x and d_y represent respectively the space between parallel antenna element in the x and y axes

In the case of 3D vehicular Massive MIMO antenna, the large-scale antenna is situated in each vehicle surface and the incident signal are transmitted in diverse direction. In consequence, the signal delay $a_{mno}(\alpha_A, \beta_E)$ by the transmitter are very different when the value of mno antenna element change, that means $mno = 1,2, \dots, N_T$.
The path delay, $a_{mno}(\alpha_A, \beta_E)$, is given by:

$$a_{mno}(\alpha_A,\beta_E)=\begin{cases} exp\begin{Bmatrix} jk_w md_x\cos\alpha_A\beta_E + j\,k_w nd_y\sin\alpha_A \\ \cos\beta_E + jk_w H\sin\beta_E \end{Bmatrix} \\ exp\begin{Bmatrix} jk_w(\mathrm{M}-1)dx\cos\alpha_A\beta_E + j\,k_w nd_y\sin\alpha_A \\ \cos\beta_E + jk_w(o-MN)d_z\sin\beta_E \end{Bmatrix} \\ exp\begin{Bmatrix} jk_w nd_y\sin\alpha_A\cos\beta_E + j\,k_w \\ (o-MN-NO)d_z\sin\beta_E \end{Bmatrix} \\ exp\begin{Bmatrix} jk_w md_x\cos\alpha_A\beta_E + j\,k_w \\ (o-MN-2NO)d_z\sin\beta_E \end{Bmatrix} \\ exp\begin{Bmatrix} jk_w md_x\cos\alpha_A\beta_E + j\,k_w Nd_y\sin\alpha_A \\ \cos\beta_E + jk_w(o-MN-2NO-MN)d_z\sin\beta_E \end{Bmatrix} \end{cases} \quad (10)$$

The channel impulse response is given by:

$$h(t)=\sum_{j=1}^{N_T}\alpha_j(t)\cdot a(\alpha_A,\beta_E) \quad (11)$$

Where $\alpha_j(t)$ is the amplitude

$a(\alpha_A,\beta_E)$ the phase shifts

N_T the total number of transmitter antenna

α_A the azimuth angles

β_E the elevation angles

By using (11), the complexes channel impulse response, between the $n_t{}^{th}$ transmitter antenna and the $n_r{}^{th}$ receiver antenna is given by:

$$h_{l,n\ \ n_r}(t)=\sum_{n=1}^{N} a_{l,n_t n_r,n}(t)\, e^{j\left(\psi_{l,n_t n_r,n}-\frac{2\pi f_c D_{l,n_t n_r,n}(t)}{c}\right)}\ \ N_C \times e^{j2\pi f_{d,l,n_t n_r,n}(t)} \quad (12)$$

Where $a_{l,n_t n_r,n}(t)$ the amplitude

$\psi_{l,n_t n_r,n}$ the phase

$D_{l,n_t n_r,n}(t)$ the distance between the l^{th} in the n^{th} cluster

N_C the total number of cluster

c the light velocity

$e^{j\left(\psi_{l,pq,n}-\frac{2\pi f_c D_{l,n_t n_r,n}(t)}{c}\right)}$ the Doppler frequency

The Doppler frequency can be written by:

$$e^{j\left(\psi_{l,n_t n_r,n}-\frac{2\pi f_c D_{l,n_t n_r,n}(t)}{c}\right)}=e^{\frac{j2\pi t v_T}{\lambda\cos\left(\alpha_{T_{n_t,l,n}}(t)-n_T\right)\cos\beta_{T_{n_t,l,n}}(t)}}\times e^{j2\pi t v_R/\lambda\cos\left(\alpha_{R_{n_r,l,n}}(t)-n_R\right)cos\beta_{R_{n_r,l,n}}(t)} \quad (13)$$

Where $\alpha_{T_{n_t,l,n}}(t)$, $\beta_{T_{n_t,l,n}}(t)$, $\alpha_{R_{n_r,l,n}}(t)$ and $\beta_{R_{n_r,l,n}}(t)$ represent the azimuth angle of departure variation, the elevation angle of arrival, the azimuth angle of arrival

λ the wavelength

v_T and v_R the speed of M and N

n_T and n_R the direction of M and N

6. Result of simulation

6.1 Signal power of 3D-Massive MIMO system

The radio propagation depends basically of the difference between the transmitter antenna high and the receiver [3].

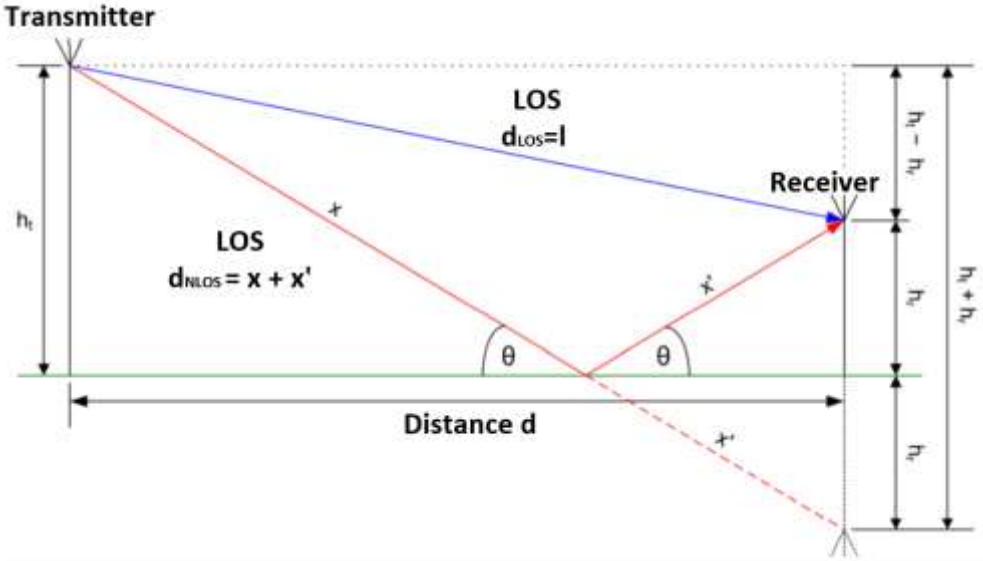

Figure 09 : Signal propagation model

The received signal power P_r is given by:

$$P_r = Pt * Gr * \frac{\lambda^2}{(4\pi D)^2} * 4[\sin((2\pi * Ht * Hr)/(\lambda * D))]^2 \quad (14)$$

As $D^2 \gg (2\pi * Ht * Hr)/\lambda$

Then

$$P_r = Pt * Gr * (Ht * Hr)^2/D^4$$

Where: Gr the received antenna gain

λ the wavelength

D the distance between the transmitter and receiver

The conditions that we have taken into accompt for a frequency range less than 6GHz is represented by the Table 02.

Table 02: Used parameters for a sub 6GHz band

	High(m)	**EIRP (dBm)**	**Gain(dBpi)**
gNB	25	46	18
Vehicle antenna	1.5	33	4

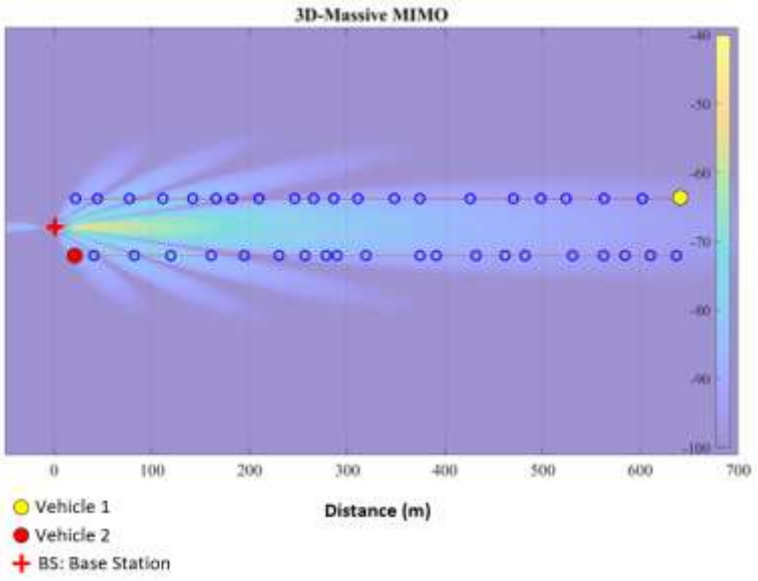

Figure 10: 3D-vehicular Massive MIMO Signal propagation power

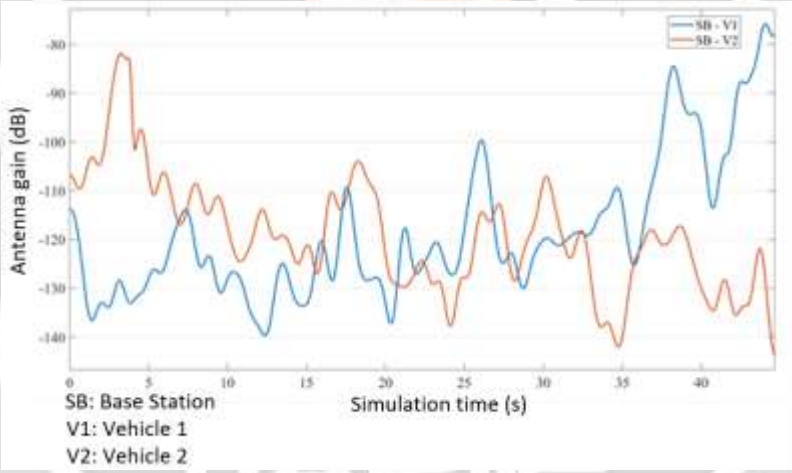

Figure 11: Vehicular Massive MIMO antenna gain for 3,5Ghz frequency band

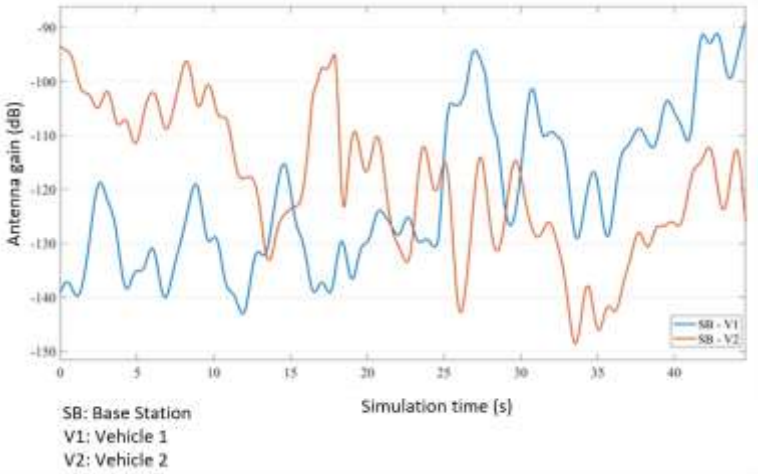

Figure 12: 3D-Massive MIMO antenna gain for 3,5Ghz frequency band

The Figure 11 and the Figure 12 show that the use of 3D-Massive MIMO antenna system give more antenna gain than the traditional Massive MIMO antenna system.

6.2 Performance evaluation of vehicle to vehicle communication

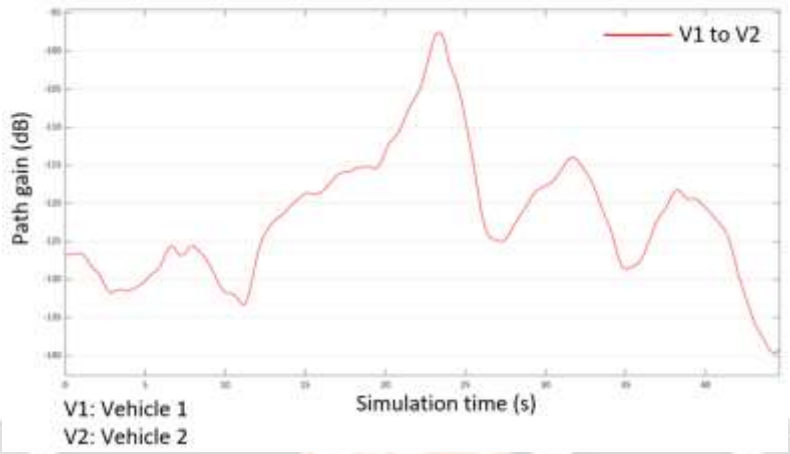

Figure 13: Massive MIMO antenna gain for V2V communication in a LOS environment and for 5,9GHz band

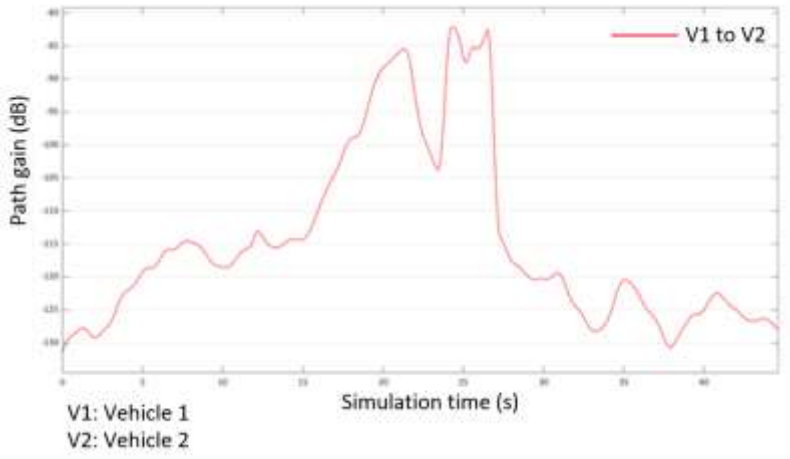

Figure 14: 3D-Massive MIMO antenna gain for V2V communication in a LOS environment and for 5,9GHz band

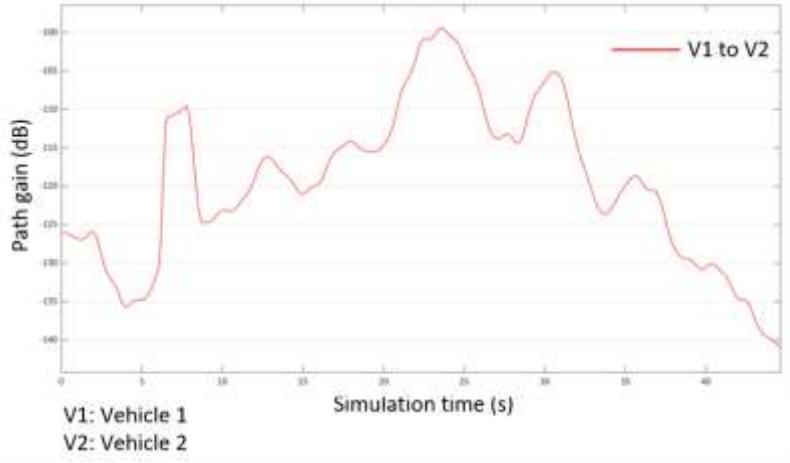

Figure 15: Massive MIMO antenna gain for V2V communication in a NLOS environment and for 5,9GHz band

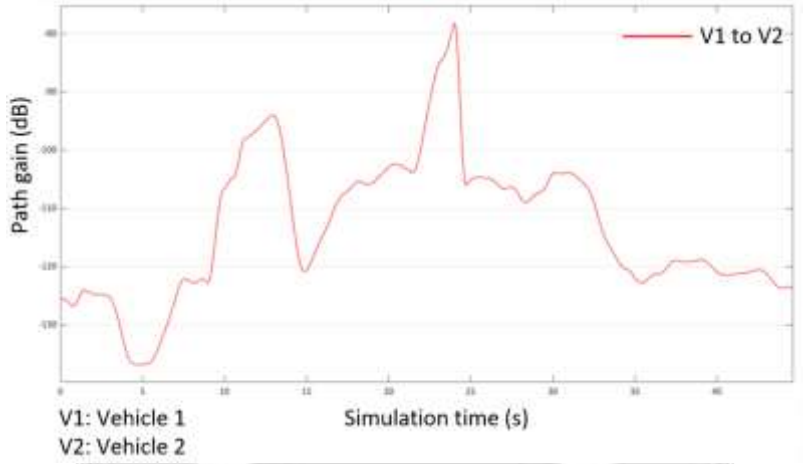

Figure 16: 3D-Massive MIMO antenna gain for V2V communication in a NLOS environment and for 5,9GHz band

Table 03: Analysis of path gain for a V2V communication

Parameters			**Path Gain(dB)**	
Scénario	**Zone**	***f*** **(GHz)**	**Massive MIMO**	**3D-Massive MIMO**
Urbain macro	LOS	5,9	-82	-98
	NLOS		-78	-100

From Table 03, we see that the power decrease when the distance between the transmitter and the receiver inceaser. In other hand, the use of 3D-Massive MIMO can help having more antenna gain than using a traditional Massive MIMO antenna.

7. CONCLUSION

In this article, we have seen the representation of the general architecture of 5G network and also the architecture of 5G vehicular network. Furthermore, this work has given a simulation result from the performance evaluation of 3D-vehicular Massive MIMO antenna compared to the traditional vehicular Massive MIMO antenna system.

8. REFERENCES

[1]. Y. Wu, H. Huang, C. Wang, Y. Pan, *"5G Enabled Internet Of Thing"*, CRC Press,2019
[2]. Laurent Gallo (Orange), Massimo Condoluci (Ericsson), "Final Design and Evaluation of the 5G V2X System", 2019
[2]. E. Dahlman, S.Parvall, J.Sköld, " *5G NR: The Next Generation Wireless Access ",* Academic Press, 2018
[3]. Hao Jiang Guan Gui, "*Channel Modeling in 5G Wireless Communication Systems*", Springer, 2020
[4]. Laurent Gallo (Orange), Massimo Condoluci (Ericsson), " *Final Design and Evaluation of the 5G V2X System Level Architecture and Security Framework*", 2019